Jan Boyke Schönborn | Bernd Hartke

Photochemical dynamics of E-methylfurylfulgide

kinematic effects on photorelaxation dynamics of furylfulgides

Suggested citation referring to the original publication:
Phys.Chem.Chem.Phys. 16 (2013), pp. 2483–2490
DOI http://dx.doi.org/10.1039/c3cp53495b

PCCP

PAPER

View Article Online
View Journal | View Issue

Cite this: *Phys. Chem. Chem. Phys.*, 2014, **16**, 2483

Photochemical dynamics of *E*-methylfurylfulgide—kinematic effects on photorelaxation dynamics of furylfulgides†

Jan Boyke Schönborn[a] and Bernd Hartke*[b]

Received 16th August 2013,
Accepted 21st November 2013

DOI: 10.1039/c3cp53495b

www.rsc.org/pccp

With the present theoretical study of the photochemical switching of *E*-methylfurylfulgide we contribute an important step towards the understanding of the photochemical processes in furylfulgide-related molecules. We have carried out large-scale, full-dimensional direct semiempirical configuration-interaction surface-hopping dynamics of the photoinduced ring-closure reaction. Simulated static and dynamical UV/Vis-spectra show good agreement with experimental data of the same molecule. By a careful investigation of our dynamical data, we were able to identify marked differences to the dynamics of the previously studied *E*-isopropylfurylfulgide. With our simulations we can not only reproduce the experimentally observed quantum yield differences qualitatively but we can also pinpoint two reasons for them: kinematics and pre-orientation. With our analysis, we thus offer straightforward molecular explanations for the high sensitivity of the photodynamics towards seemingly minor changes in molecular constitution. Beyond the realm of furylfulgides, these insights provide additional guidance to the rational design of photochemically switchable molecules.

1 Introduction

Bistable molecules that can be switched photochemically are of strong interest as central units in various applications such as light-driven molecular motors[1,2] or optical data storage.[3] Furylfulgides are a well-known class of these compounds.[4] The intended photochemical switching in this class of molecules is between an open (E) and a cyclic (C) form, which can be photoexcited by different wavelengths. Both forms are thermally stable, and the molecules exhibit only little photochemical fatigue. In addition to the intended E → C conversion, the *E* isomers of various furylfulgides can photorelax by isomerisation at the double bond between C3 and C4 (*cf.* Fig. 1) to form the *Z* isomer. This reaction competes with the wanted cyclisation in a destructive fashion since the *Z* isomer cannot directly be transformed into the *C* isomer but has to be excited to form the *E* isomer first. In this article, we will present a detailed theoretical study of the photorelaxation dynamics of the *E* isomer of methylfurylfulgide (Fig. 1a) and compare the results with the data from a previous study[5] of isopropylfurylfulgide (the same molecule as in Fig. 1a except for an isopropyl group at atom C3 instead of the methyl group). We will use this comparison to show the pronounced effects that even seemingly minor substitution changes have on the de-excitation dynamics.

2 Summary of known experimental and theoretical data

Various articles have been dedicated to the study of the switching properties of furylfulgides in different media such as films[6] and crystals.[7,8] As can be expected from the potential importance of furylfulgides as molecular switches, there have been many experimental studies on these. Here, we will only be citing a subjective selection of experiments that focus on the unravelling of the underlying mechanisms.

In this paragraph, we mention work reported by the Temps group. Large parts of it were done in direct collaboration with our group, with frequent cross-fertilization of ideas and interpretations, running in both directions. Photodynamics of *Z*-methylfurylfulgide were studied by Renth *et al.*[9] who observed ultrafast dynamics and strongly damped coherence. The subject of the present article was experimentally studied by Siewertsen *et al.*[10] who observed ultrafast dynamics with two time constants of 100 and 250 fs, respectively. These were tentatively assigned to the formation of the *C* and the *Z* isomer. In spite of rigorous analysis, the authors were not able to definitely decide between two explanatory models. In the first

[a] *Institut für Chemie, Universität Potsdam, Karl-Liebknecht-Straße 24-25, D–14476 Potsdam-Golm, Germany*
[b] *Institut für Physikalische Chemie, Christian-Albrechts-Universität, Olshausenstraße 40, D–24098 Kiel, Germany. E-mail: hartke@pctc.uni-kiel.de*

† Electronic supplementary information (ESI) available. See DOI: 10.1039/c3cp53495b

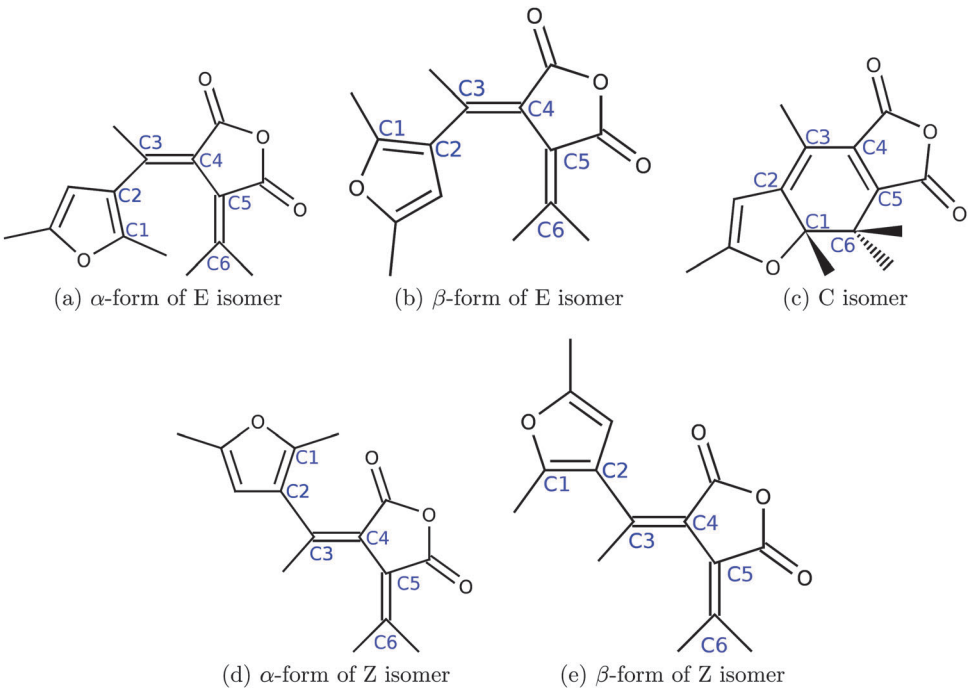

Fig. 1 Reactant (E), product (C), and unwanted side product (Z) of the present study. The atoms forming the central hexatriene–cyclohexadiene unit are labeled in blue.

model, they assumed two distinct excitation–de-excitation paths in which E_α (Fig. 1a) de-excites towards C (Fig. 1c) and E_β (Fig. 1b) de-excites towards Z_β (Fig. 1e). In the second model, only the more abundant E_α conformer is excited. The excited-state wavepacket then splits to form C (Fig. 1c) and Z_α (Fig. 1d). In later studies, Siewertsen *et al.*[11,12] supported the second model of a split de-excitation pathway for the dominant E_α conformer, which was further confirmed by a theoretical study of *E*-isopropylfurylfulgide[5] by the present authors.

Other groups have examined similar systems with similar methods. The ring opening and closing reactions of indolylfulgimide were studied by Koller *et al.*[13] *via* femtosecond vibrational spectroscopy. They reported ultrafast dynamics, in which the ring closure was faster (500 fs time constant) than the ring opening (2–4 ps). For indolylfulgide, Cordes *et al.*[14] reported the ring opening reaction to happen *via* two different conical intersections with a notable influence of solvent and of excitation wavelength. The ring closure, on the other hand, appears to happen *via* a simple barrierless path with little effect of either solvent or excitation energy. In a study of triflourinated indolylfulgide, Draxler *et al.*[15] were able to show that the efficiency of the ring opening reaction can be increased massively by a ring closure reaction preceding directly.

Besides the previously reported study of the photorelaxation dynamics of *E*-isopropylfurylfulgide,[5] there have been some other theoretical investigations of furylfulgides. Frequency-dependent hyperpolarizabilities were calculated using TDDFT by Seal and Chakrabarti,[16] providing some explanation for the switching properties of furylfulgides. In a study using UHF and CASSCF calculations in a 6-31G(d) basis set, Yoshioka *et al.*[17] studied ground-state isomerisation paths concluding that a CASSCF(8,8) is the minimal active space for a reasonable description of these. Tomasello *et al.*[18] highlighted the zwitterionic character of the first excited state of methylfurylfulgide close to the conical intersection that facilitates the ring closure. This presented key information to abandon the cyclohexadiene–hexatriene system as a model for more complex, distantly related systems like furylfulgides.

In this article, we will present a detailed study of full-dimensional photo-de-excitation dynamics of *E*-methylfurylfulgide. It complements our earlier study on *E*-isopropylfurylfulgide[5] and it substantiates and extends the mechanistic hypotheses presented by our experimental collaboration partners in ref. 12.

3 Computational approach

3.1 Methods and technical details

The simulation of the photochemical processes of *E*-methylfurylfulgide was done by use of semiclassical direct molecular dynamics as implemented in the MNDO program.[19] The electronic structure calculations were carried out using the semiempirical OM3 method[20–22] and a multi-reference configuration interaction (MR-CI) treatment[23] based on the graphical unitary group approach. Nuclear motion was represented by quasi-classical trajectories, by use of Tully's surface hopping approach with the fewest switching algorithm.[24,25]

This semiempirical MR-CI approach provides a good compromise between computational expense and accuracy in excited-state dynamics simulations. This has been shown in

various recent studies for a broad variety of systems.[26–35] The most important study for this specific system clearly is the study of *E*-isopropylfurylfulgide presented in ref. 5. Based on the very close relation between these two furylfulgides, one can expect a similar degree of reliability of the OM3-MRCI description. Nevertheless, we do present a direct comparison of OM3-MRCI data to multireference *ab initio* data for a small but relevant and arbitrary selection of structures in the ESI.†[36]

The MR-CI treatment of *E*-methylfurylfulgide consisted of an active space of 18 electrons in 17 orbitals. The orbitals were the ones with the largest π-character at the carbon and oxygen atoms in the conjugated system (*i.e.*, all carbon atoms except the ones in the methyl groups, and all oxygen atoms, a total of 14 atoms). Although this active space is larger than a formal π-space of the system, the fact that the model uses canonical orbitals causes the π-character to spread over more orbitals than the ones that would be needed in a minimal representation. Choosing the orbitals by their π-character with respect to the conjugated system and the size of the active space yields reasonable results, which is sufficient to justify their use in the semiempirical model. Once chosen, the character of these orbitals was tracked throughout the simulation to keep a consistent active space. The closed-shell ground-state configuration and the HOMO–LUMO singly and doubly excited configurations were used as reference configurations, from which all single and double excitations where included. The six lowest singlet states were treated for the calculation of the spectra.

More trajectories were simulated for the α-isomer than for the less abundant[12] β-isomer (see Fig. 1 for the structures). The total numbers are given in Sections 4.1 and 4.2.

The dynamics were simulated for an isolated molecule with a time step of 0.1 fs. Prior to the actual de-excitation dynamics, the ground-state structure was thermalized at 300 K with a velocity-scaling thermostat acting every 100 steps for 1500 steps. Although this is not long enough for large-scale motions to happen, it is still sufficient time, since we simulate the relevant isomers separately and do not need to sample their equilibrium thermally. After the thermalisation, the final structure was used as input structure for the de-excitation dynamics (15 000 time steps for the α isomer, 11 000 for the β isomer), starting on the first excited state with starting velocities corresponding to 300 K. No thermostat was used in these production runs. Some of the de-excitation trajectories were started from thermalization runs that only treated three electronic states. This does not affect their use for thermalization, since the representation of the ground state does not change, but prohibits their use in static spectra. We note this here to explain why we were able to start more de-excitation trajectories than the ones we used for the calculation of the static spectra.

Spectra were calculated from the trajectories by use of transition dipole moments and transition energies for the six energetically lowest states. For calculation of static spectra the time information in the trajectories was ignored, while it was kept for the transient spectra (see ESI† in ref. 36 for more details on the applied procedure). To facilitate optical comparison of the experimental and theoretical spectra, the calculated spectra were convoluted with a Gaussian-shaped resolution function of widths 50 fs and 20 nm.

4 Results

4.1 Simulated static UV/Vis spectrum

Static UV/Vis spectra were calculated from the thermalisation runs (139 for the α- and 55 for the β-isomer) as detailed in Section 3.1 and in the ESI.† The spectra of the isomers where weighted 2α : 1β as published in ref. 12. The weighted spectrum is depicted in Fig. 2 together with the replotted original data from ref. 12 for easier comparison. The spectra show excellent agreement between the experimental and the theoretical data. The lack of short wavelength signals is expected due to the lack of electronically excited states above S_5. The major difference thus occurs in the second band. The second band in the simulated spectrum is too intense compared to the first one and is relatively broad. Underlying this band are two distinct absorption signals; the high-energy one is formed by the S_4- and S_5-state. Hence, the most likely explanation for the differences is that the fourth and fifth excited states are predicted to be too low in energy. In any case, as before for isopropylfurylfulgide, the most significant error, besides the shift, occurs in highly excited states which have impact on the calculated spectra but none on the de-excitation dynamics. As expected, the simulated static spectrum of *E*-methylfurylfulgide is in equally good agreement with the experimental spectrum as already observed for *E*-isopropylfurylfulgide.[5]

4.2 Simulated transient UV/Vis spectra

Time-resolved spectra were calculated from the de-excitation trajectories (156 α and 67 β) as explained in Section 3.1. The resulting transient absorption maps are given in Fig. 3, together with the replotted original data from ref. 12. At short times (about 100 fs) there are two signals in the experimental spectrum that do not appear in the simulation: a more intense one between 350 and 400 nm and a less intense one around 500 nm.

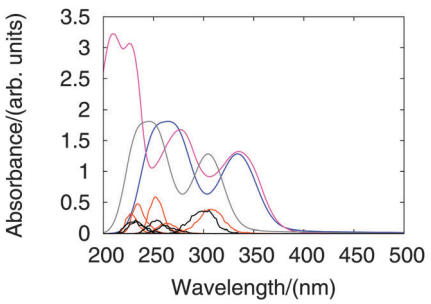

Fig. 2 Simulated (blue) and experimental (measured in *n*-hexane) (magenta) static spectra of *E*-methylfurylfulgide (Fig. 1a and b). Original data that were also shown in different form in ref. 12 were replotted for the experimental spectrum. The simulated spectrum was redshifted by 2900 cm^{-1} for easier comparison. The unshifted simulated spectrum is depicted in grey, and the underlying transitions are given in orange, for the α-, and black, for the β-isomer. The relative intensities of the signals of the two isomers are consistent with their respective abundance.

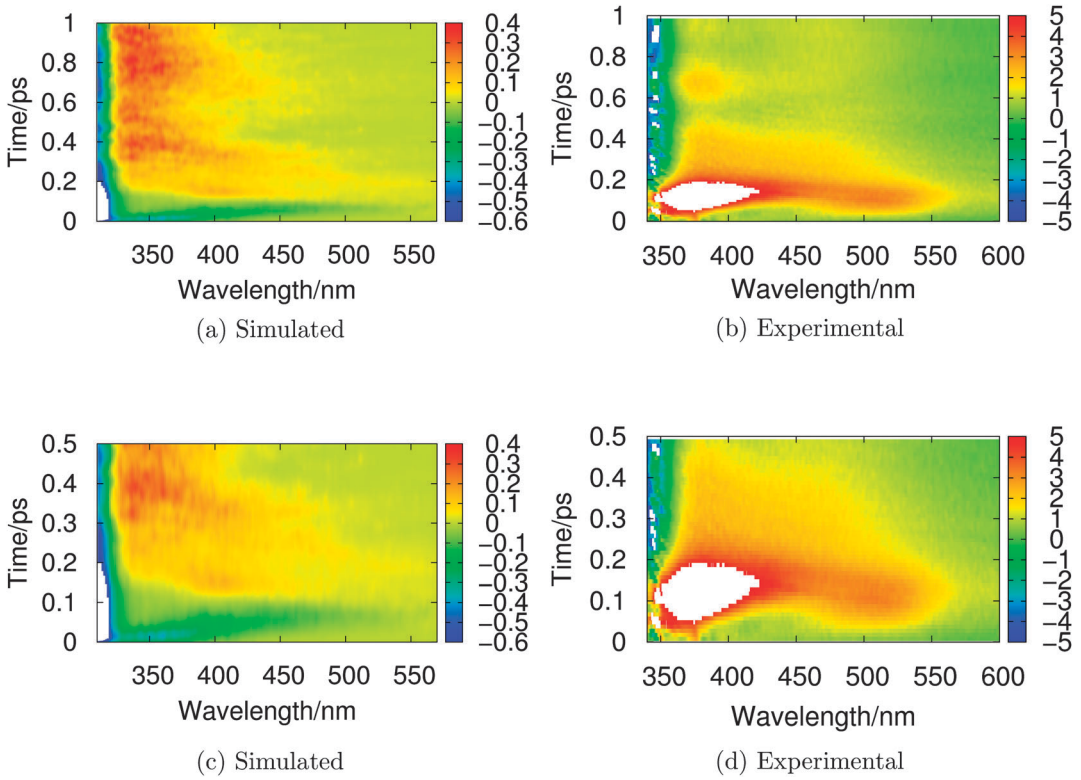

Fig. 3 Simulated (left column) and experimental spectra (right column; replotted from original data[12]) for 1.0 ps (top row) and up to 0.5 ps (bottom row) for detailed comparison.

Both of these are usually attributed to excited state absorption. Since the simulation could not account for highly excited states, there are no electronic states to which an excitation in that energetic region could happen. Thus these signals do not appear in the simulation for essentially the same reasons as the high energy signals in the static spectrum. The most important difference between simulated and experimental spectra is the intense feature that takes up the left-hand side of the spectrum. The discrepancy is most pronounced for the oscillatory feature at short wavelengths and late times (around 0.7 to 0.8 ps). On the other hand especially at this point in time the traces of this oscillation show up in the experimental spectrum. This part of the spectrum is caused by hot reactant (Fig. 1a and b) and by formation of the *Z*-isomer (Fig. 1d and e). Underlying this signal is an ample movement of the molecule, which causes the spectral oscillation. It is straightforward to expect this oscillation to be efficiently damped by solvent which is absent in the simulation. Additionally, the lack of solvent in the simulation favours the formation of the *Z*-isomer, by a factor of roughly four (see Section 4.3), which has absorption signals further to the red than the *E*-isomer, which strongly enhances the discrepancy. In any case, the process that causes the difference happens on the ground state after the relaxation is over. Thus, as already stated for isopropylfurylfulgide,[5] it is reasonable to check whether the actual de-excitation process is represented qualitatively correctly, although the final outcome shows some disagreement. For this reason, the spectra were replotted up to only 0.5 ps (second row in Fig. 3). This interval covers the de-excitation and the ground state dynamics ensuing directly afterwards. Here the spectra fit extremely well, except for the excited state absorption signals at 375 nm and 525 nm. As pointed out previously, both are absent in the simulation because their final state is beyond S_5 and thus not part of the simulation. In between these two signals there is a part of lower intensity in the experimental spectrum which fits well with the signature of the stimulated emission feature in the simulated spectrum. The step-like feature at about 450 nm in the simulation and 500 nm in the experiment that occurs at around 0.3 ps in both spectra especially highlights the excellent agreement. This structure is a region of positive change in optical density that has the outline of a step in time and wavelength. Pictorially speaking, the step goes from about 0.2 ps to about 0.4 ps, and from 320 to 500 nm, in a slanted fashion. This is a very important piece of agreement between the simulated spectrum and the experimental one. Taking into account the very good comparability of both static and transient spectral data, an analysis of the underlying dynamics is sufficiently justified.

4.3 Photoisomerisation reaction dynamics

The analysis of the photo-relaxation will be focused on the α-rotamer since it features the competing relaxation mechanisms. As already stated for *E*-isopropylfurylfulgide, the β-rotamer relaxes only *via* the central ethylenic pathway. Overall, *E*-methylfurylfulgide shows the same principal conical intersection (CoIn) types as already observed in the dynamics of *E*-isopropylfurylfulgide[5] and optimised for related molecules.[37] Fig. 4a–c show a qualitative depiction of the prototypical CoIns involved in the relaxation.

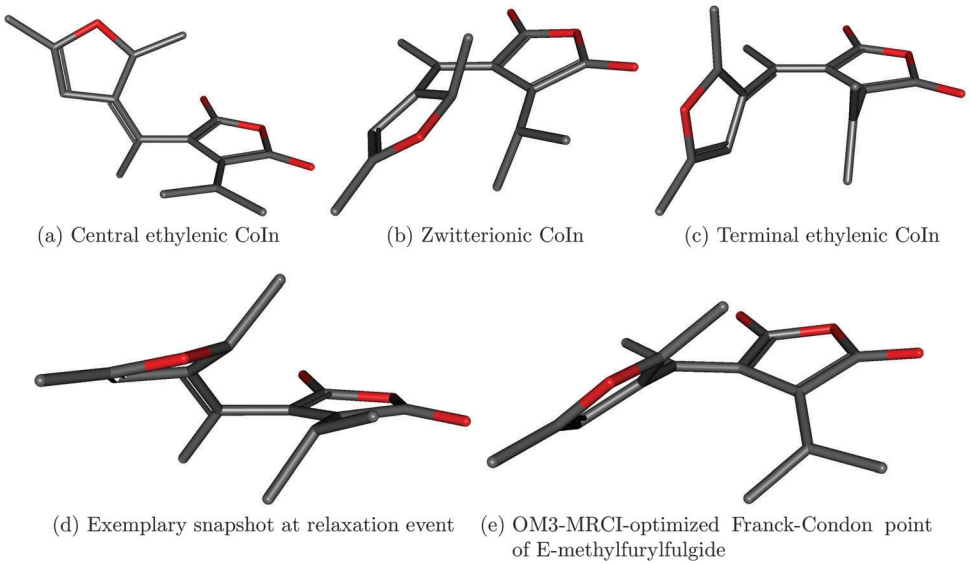

Fig. 4 Qualitative depiction of the three prototypical CoIns (a–c) relevant to the relaxation of *E*-methylfurylfulgide, an exemplary structure (d), showing the mixing of the structures (a and b) in the actual dynamics, and the OM3-MRCI-optimized Franck–Condon point (e). Hydrogen atoms are left out for easier perception of the structures.

As already found for *E*-isopropylfurylfulgide, the actual structures at the electronic de-excitation events differ significantly from the prototypical structures and more resemble a mixture of these. To highlight this point, we also depict an exemplary structure at the surface transition in Fig. 4d. This structure excellently shows how the progression along the zwitterionic pathway causes the furyl ring to tilt down and not follow the movement caused by the progression along the central ethylenic pathway. The depicted structure is a rather pronounced example used to make the point clear. There are trajectories in which the process is less obvious. The paths include a zwitterionic CoIn facilitating the ring closure (happening basically by shortening of the distance between C1 and C6; see Fig. 1 for the numbering), a CoIn happening around the central double bond between C3 and C4 and one at the terminal double bond between C5 and C6. Although the paths are the same, they occur with significantly different relative likelihood. In Table 1 the relative importance of the different paths is given for *E*-methylfurylfulgide and *E*-isopropylfurylfulgide (the data of which are taken from ref. 5). We attributed the trajectories of the α-isomer to the paths by analysing the structure at the point of surface transition with respect to the characteristic coordinates as specified in Fig. 5d. The trajectories were attributed to a path where the value of the characteristic coordinate is within a certain tolerance interval at the point of the surface transition (for methylfurylfulgide these are: 1.20 Å $< r_1 <$ 2.55 Å; 75° $< \phi_1 <$ 105°; 80° $< \phi_2 <$ 100°).

Table 1 Percentage of excited-state trajectories of α-isomers relaxing *via* the three different CoIn types. Data for *E*-isopropylfurylfulgide were taken from ref. 5

Molecule	Zwitterionic CoIn	Central CoIn	Terminal CoIn
E-Methylfurylfulgide	16%	80%	3%
E-Isopropylfurylfulgide	68%	16%	16%

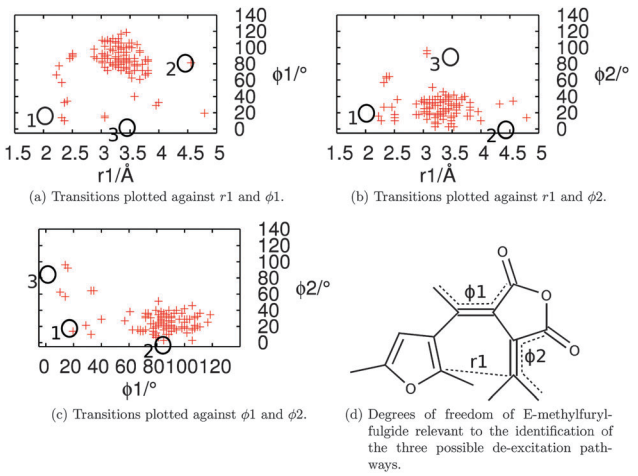

Fig. 5 Location of $S_0 \leftarrow S_1$ transitions in internal coordinates identifying de-excitation paths (a–c). Approximate locations of the optimised CoIns are given by black circles (1: pericyclic, 2: central ethylenic, 3: terminal ethylenic). The coordinates are given in (d).

These values were chosen with the specific aim of characterizing all trajectories and minimizing double identifications. In cases of double positives or all negatives, the respective trajectories were inspected by eye and attributed to a path. From this analysis we calculated the percentages given in Table 1. Since the simulation is dynamic and the paths mix during the relaxation (see Fig. 4d and ref. 5 for details), the assignment is somewhat ambiguous but can be taken to be qualitatively correct. A less ambiguous way of depicting the importance of the different paths is given in Fig. 5a–c. Here, the locations of points at which trajectories cross from the excited to the ground state are given with respect to three coordinates that can be used to qualitatively differentiate between the three CoIns (the coordinates are given in Fig. 5d). In these plots, the dominant role of

the central ethylenic CoIn (characterised by ϕ_1) is evident. The de-excitation events cluster and do so closest to the region of the central ethylenic CoIn compared to the other two (for values of comparable molecules see ref. 5 and 37). This is strikingly different from *E*-isopropylfurylfulgide where the de-excitation events scatter between all relevant CoIns.[5]

The de-excitation dynamics lead to a quantum yield of 0.54 (0.43 in pure α) for the $E \rightarrow Z$ isomerisation and 0.03 (0.04 in pure α) for the cyclisation. These quantum yields are distorted in favour of the $E \rightarrow Z$ isomerisation in comparison to the experiment,[12] which are 0.14 (E → Z) and 0.23 (E → C). On the other hand, they fit well with the experimental observation that the $E \rightarrow Z$ isomerisation is more efficient in *E*-methylfurylfulgide compared to *E*-isopropylfurylfulgide, which is also true in our simulations (see ref. 5 for details on *E*-isopropylfurylfulgide). We attribute these deviations in the quantum yields to the lack of solvent in our simulation, in agreement with our previous study. Surely some part of the discrepancies is also caused by the inexact model. Due to the overall similarity of methyl- and isopropylfurylfulgide (*e.g.* see ref. 5 and 18) we believe these inaccuracies to be also similar. The $E \rightarrow Z$ isomerisation involves ample motions of the molecule that can be expected to be dampened by the solvent efficiently, while the cyclisation is likely not hampered much by the solvent. Therefore, the quantum yields are likely to be shifted in favour of the cyclisation reaction upon introduction of solvent for purely sterical reasons. This becomes very clear in Fig. 4. On the course of the $E \rightarrow Z$ isomerisation (starting from Fig. 4e), the molecule has to pass a structure similar to Fig. 4a, although it will do so on the ground state since the actual crossing point to the ground state will look more similar to Fig. 4d. The motion leading to such a structure will be hampered severely by the sorrounding solvent. In contrast, there is already a huge similarity between the zwitterionic conical intersection in Fig. 4b and the approximate starting structure in Fig. 4e. To cover the coordinate space between the two structures and then to continue to the cyclic product (not depicted here) there is probably not a lot of solvent to be displaced. On the excited state there is also an obvious differentiation between the zwitterionic and the central ethylenic character of the path. This becomes clear from Fig. 4d: the part of the molecule that dominantly goes towards the central ethylenic CoIn is the methyl group, while the C1–C6 ring closes as part of the progression toward the zwitterionic CoIn. It becomes clear from the figure that while the movement of the methyl group will have to push away solvent, the ring-closing motion will not. Obviously, none of the effects can be expected to be sufficiently large to completely close a pathway but they will influence the detailed impact the paths will have on the actual relaxation dynamics. Our line of argument is related to the discussion of volume conserving and non-conserving CoIns in green fluorescent protein[38,39] but the impact in our system is expected to be significantly smaller than the effect of a surrounding protein, and our analysis is more qualitative.

5 Kinematic and pre-orientational differentiation between *E*-methyl- and *E*-isopropylfurylfulgide

Our simulations reproduce the experimental trend that shows a strong bias towards the $E \rightarrow Z$ isomerisation in *E*-methylfurylfulgide in comparison to *E*-isopropylfurylfulgide. A detailed analysis of our trajectores allows us to understand exactly how the different substituents cause this very different relaxation behaviour. In Fig. 6, the average of the three coordinates depicted is given for the full ensembles of the α isomer trajectories of *E*-methylfurylfulgide (red) and *E*-isopropylfurylfulgide (blue). The data for *E*-isopropylfurylfulgide were taken from the simulations published in ref. 5. A comparison of the data for r_1 (Fig. 6a) shows that while both ensembles evolve towards the zwitterionic CoIn (≈2.0 Å) at approximately the same speed, the isopropylfurylfulgide has a headstart: it begins at about 3.5 Å and decreases to about 2.5 Å, compared to a starting point of about 3.7 Å for methylfurylfulgide that reaches its turning point close to 3.2 Å. In the latter parts, the thus far parallel evolution splits when the formation of the cyclic product sets in isopropylfurylfulgide, while methylfurylfulgide is virtually unreactive in this respect. Analysis of Fig. 6b does not show a significant difference at the starting value of ϕ_1 but reveals the speed of the progression along that coordinate to be very different for the two molecules. This leads to methylfurylfulgide approaching the region of the central ethylenic CoIn around 90° much faster than isopropylfurylfulgide.

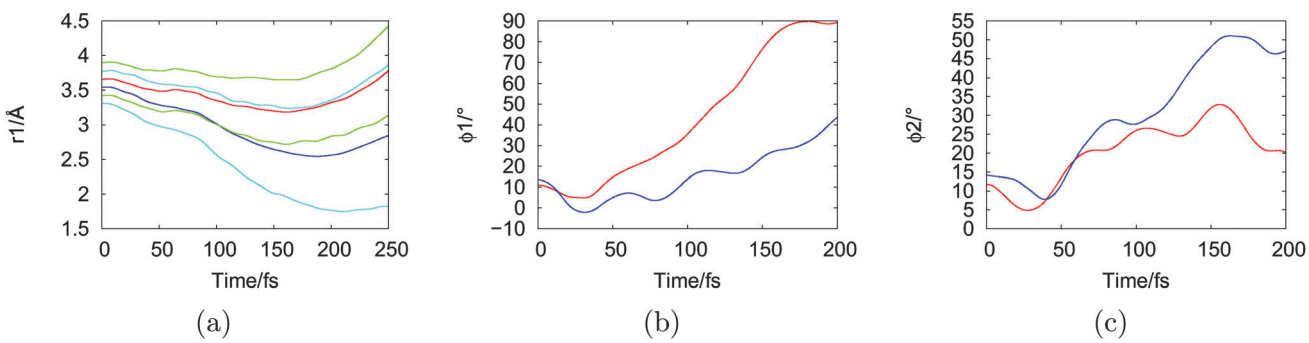

Fig. 6 Average values of the reaction-path characteristic coordinates (r_1: a, ϕ_1: b and ϕ_2: c) during the first 250 fs of the photo-de-excitation of *E*-methylfurylfulgide (red) and *E*-isopropylfurylfulgide (blue). In (a) the standard deviation is given (methyl: green and isopropyl: light-blue).

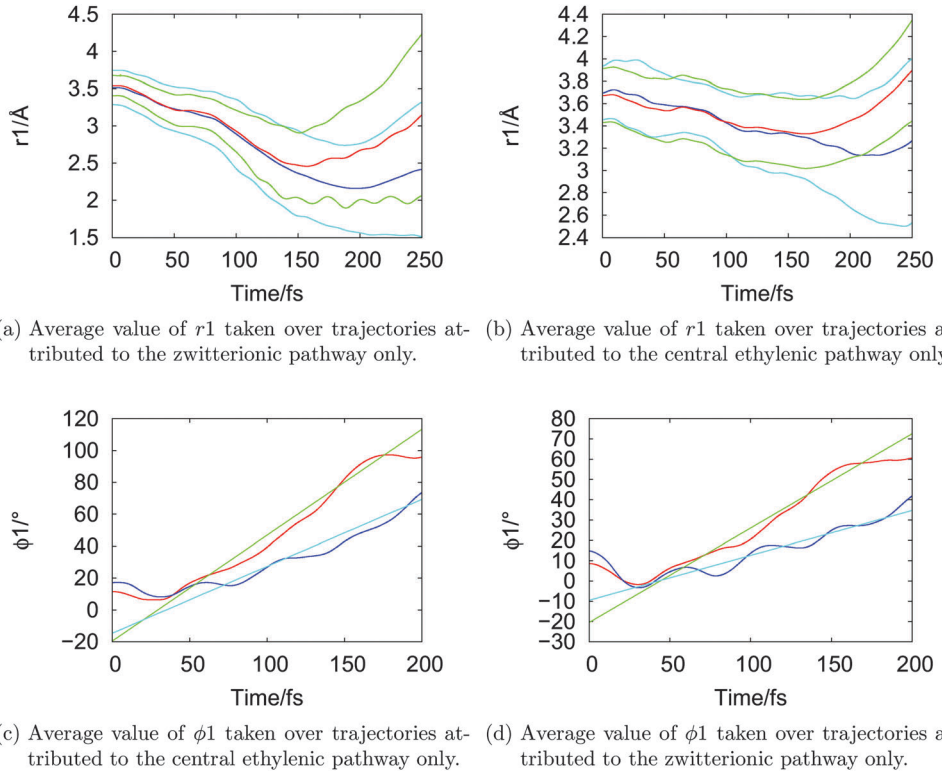

(a) Average value of $r1$ taken over trajectories attributed to the zwitterionic pathway only.

(b) Average value of $r1$ taken over trajectories attributed to the central ethylenic pathway only.

(c) Average value of $\phi1$ taken over trajectories attributed to the central ethylenic pathway only.

(d) Average value of $\phi1$ taken over trajectories attributed to the zwitterionic pathway only.

Fig. 7 Average values of the reaction-path characteristic coordinates (r_1: a and b ϕ_1: c and d) during the first 250 fs of the photo-de-excitation of *E*-methylfurylfulgide (red) and *E*-isopropylfurylfulgide (blue). In (a) and (b) standard deviations are given in green for methyl- and light-blue for isopropylfurylfulgide and (c) and (d) give corresponding linear regressions (green and light-blue respectively).

Fig. 6c shows no significant differences below 100 fs. After that the second increase setting in at about 100 fs in isopropylfurylfulgide is not due to isomerisation along this path. It is caused by the beginning of formation of the cyclic product which causes pyramidalisation of C6 and thus opens the angle ϕ_2. This is not a change connected to the path of interest for this coordinate and will therefore not be discussed further. To further investigate the features observed for r_1 and ϕ_1, the trajectories of both methyl- and isopropylfurylfulgide from these paths were separated into groups that are reactive and unreactive with respect to the specific reaction (cyclisation for r_1 and $E \rightarrow Z$ isomerisation for ϕ_1). For these groups, the average of the characteristic coordinates was calculated. Fig. 7 depicts the evolution of these averages over time. For easier comparison, the mostly linear parts of the graphs were analysed by linear regressions that are also given in the plots. The graphs for the r_1 coordinate (Fig. 7a and b) show that trajectories of both molecules that form the cyclic product start off from comparable values of r_1 of about 3.5 Å, while unreactive ones have an average starting value of 3.7 Å. Together with the difference in the average of the full ensemble this proves a pre-orientational effect by the isopropylgroup that favours ring formation. As visible from the standard deviation the effect of the pre-orientation is not strong enough not to allow for some overlap. This is not unexpected since not only the starting geometry (especially in only one coordinate) is relevant to the details of the photo-relaxation process. The data nevertheless show that the zwitterionic pathway is favored by the ground-state ensemble of isopropylfurylfulgide. The data for ϕ_1 do not show significant differences in starting values, neither for reactive–unreactive trajectories nor for different substitution. The faster progression of methylfurylfulgide towards the CoIn persists in both reactive and unreactive trajectories. From the linear regressions, the speed of the evolution along ϕ_1 can be extracted. For methylfurylfulgide the speed is 0.66° fs^{-1} for reactive and 0.46° fs^{-1} for unreactive trajectories, while for isopropylfurylfulgide it is 0.42° fs^{-1} and 0.22° fs^{-1}. Thus, in this case it is evident that the methyl group kinematically favours the $E \rightarrow Z$ isomerisation compared to the isopropyl group.

6 Summary and conclusions

In this article, we have presented the first full-dimensional study of the de-excitation dynamics of *E*-methylfurylfulgide, and we arrive at good agreement with experiment. The CoIns that are relevant here are the same as the ones active in *E*-isopropylfurylfulgide (and they are prototypical in the relaxation of furylfulgides, see ref. 5 and 37). However, in direct comparison between *E*-methylfurylfulgide and *E*-isopropylfurylfulgide, the detailed dynamics cause significantly different relative importance of these CoIns and thus different quantum yields for the respective reaction products. Qualitatively, this quantum yield difference is also in agreement with experiment. By a

comparative analysis of the trajectories for both isopropyl- and methylfurylfulgide, we were able to attribute the differences to a twofold reason: (1) a pre-orientation in the isopropylfurylfulgide that facilitates ring closure (as already suggested by Siewertsen *et al.*[12]); (2) a kinematic effect that causes the methylfurylfulgide to reach the region of the CoIn seam that facilitates the $E \rightarrow Z$ isomerisation much more efficiently than the isopropylfurylfulgide. By our study we were able to make an important step in the theoretical study of substitution effects of furylfulgides, in which seemingly minor and/or peripheral changes show pronounced effects. Together with our previous work on *E*-isopropylfurylfulgide[5] and with the work of our experimental collaboration partners,[9–12] significant steps have been made towards rational design of photochemical molecular switches.

Based on our insights gained in this study and in previous ones, we plan to investigate further furylfulgides to uncover more connections between substituent effects (kinematic, pre-orientational, electronic, *etc.*) and dynamic preferences in photo-de-excitation, including (anti-)cooperative effects of several different substituent variations. Additionally we are currently working on incorporating the results of our investigation into the design of new molecular switches based on molecular frameworks not studied thus far.

Acknowledgements

JBS and BH thank Dr Ron Siewertsen, Dr Falk Renth and Prof. Dr Friedrich Temps for a fruitful collaboration on molecular switches, in particular for many stimulating discussions on furylfulgides and for access to experimental data prior to publication. Financial support from the German Science Foundation DFG *via* the Collaborative Research Center SFB677 ''Function by Switching'' is gratefully acknowledged.

References

1 *Molecular Switches*, ed. B. L. Feringa, Wiley-VCH, Weinheim, 2001.
2 V. Balzani, A. Credi and M. Venturi, *Molecular Machines: Concepts and Perspectives for the Nanoworld*, Wiley-VCH, Weinheim, 2008.
3 A. S. Dvornikov, Y. Liang, C. S. Cruse and P. M. Rentzepis, *J. Phys. Chem. B*, 2004, **108**, 8652–8658.
4 Y. Yokoyama, *Chem. Rev.*, 2000, **100**, 1717–1740.
5 J. B. Schönborn, A. Koslowski, W. Thiel and B. Hartke, *Phys. Chem. Chem. Phys.*, 2012, **14**, 12193.
6 R. Matsushima, T. Hayashi and M. Nishiyama, *Mol. Cryst. Liq. Cryst.*, 2000, **344**, 241.
7 L. Khedhiri, A. Corval, R. Casalegno and M. Rzaigui, *J. Phys. Chem. A*, 2004, **108**, 7473.
8 J. Harada, R. Nakajima and K. Ogawa, *J. Am. Chem. Soc.*, 2008, **130**, 7085.
9 F. Renth, M. Foca, A. Petter and F. Temps, *Chem. Phys. Lett.*, 2006, **428**, 62.
10 R. Siewertsen, F. Renth, F. Temps and F. Sönnichsen, *Phys. Chem. Chem. Phys.*, 2009, **11**, 5952.
11 F. Strübe, R. Siewertsen, F. D. Sönnichsen, F. Renth, F. Temps and J. Mattay, *Eur. J. Org. Chem.*, 2011, 1947–1955.
12 R. Siewertsen, F. Strube, J. Mattay, F. Renth and F. Temps, *Phys. Chem. Chem. Phys.*, 2011, **13**, 3800–3808.
13 F. O. Koller, W. J. Schreier, T. E. Schrader, S. Malkmus, C. Schulz, S. Dietrich, K. Rück-Braun and M. Braun, *J. Phys. Chem. A*, 2008, **112**, 210.
14 T. Cordes, T. T. Herzog, S. Malkmus, S. Draxler, T. Brust, J. A. DiGirolamo, W. J. Lees and M. Braun, *Photochem. Photobiol. Sci.*, 2009, **8**, 528.
15 S. Draxler, T. Brust, S. Malkmus, J. A. DiGirolamo, W. J. Lees, W. Zinth and M. Braun, *Phys. Chem. Chem. Phys.*, 2009, **11**, 5019.
16 P. Seal and S. Chakrabarti, *J. Phys. Chem. A*, 2010, **114**, 673.
17 Y. Yoshioka, M. Usami, M. Watanabe and K. Yamaguchi, *THEOCHEM*, 2003, **623**, 167–178.
18 G. Tomasello, M. J. Bearpark, M. A. Robb, G. Orlandi and M. Garavelli, *Angew. Chem., Int. Ed.*, 2010, **49**, 2913–2916.
19 W. Thiel, *MNDO program, version 6.1.*, Max-Planck-Institut für Kohlenforschung, Mülheim an der Ruhr, Germany, 2007.
20 W. Weber, PhD thesis, Universiät Zürich, Switzerland, 1996.
21 W. Weber and W. Thiel, *Theor. Chem. Acc.*, 2000, **103**, 495.
22 N. Otte, M. Scholten and W. Thiel, *J. Phys. Chem. A*, 2007, **111**, 5751.
23 A. Koslowski, M. Beck and W. Thiel, *J. Comput. Chem.*, 2003, **24**, 714.
24 J. C. Tully, *J. Chem. Phys.*, 1990, **93**, 1061.
25 E. Fabiano, T. W. Keal and W. Thiel, *Chem. Phys.*, 2008, **349**, 334.
26 E. Fabiano and W. Thiel, *J. Phys. Chem. A*, 2008, **112**, 6859.
27 Z. Lan, E. Fabiano and W. Thiel, *J. Phys. Chem. B*, 2009, **113**, 3548.
28 Z. Lan, E. Fabiano and W. Thiel, *ChemPhysChem*, 2009, **10**, 1225.
29 Z. Lan, Y. Lu, E. Fabiano and W. Thiel, *ChemPhysChem*, 2011, **12**, 1989.
30 Y. Lu, Z. Lan and W. Thiel, *Angew. Chem., Int. Ed.*, 2011, **50**, 6864.
31 O. Weingart, Z. Lan, A. Koslowski and W. Thiel, *J. Phys. Chem. Lett.*, 2011, **2**, 1506.
32 A. Kazaryan, Z. Lan, L. Schäfer, W. Thiel and M. Filatov, *J. Chem. Theory Comput.*, 2011, **7**, 2189.
33 G. Cui, Z. Lan and W. Thiel, *J. Am. Chem. Soc.*, 2012, **134**, 1662.
34 Z. Lan, Y. Lu, O. Weingart and W. Thiel, *J. Phys. Chem. A*, 2012, **116**, 1510.
35 Y. Lu, Z. Lan and W. Thiel, *J. Comput. Chem.*, 2012, **33**, 1225.
36 ESI†.
37 A. Nenov and R. de Vivie-Riedle, *J. Chem. Phys.*, 2011, **135**, 034304.
38 J. E. Norton and K. N. Houk, *Mol. Phys.*, 2006, **104**, 993.
39 S. L. Maddalo and M. Zimmer, *Photochem. Photobiol.*, 2006, **82**, 367.

